This article has been accepted for publication in a future issue of this journal, but has not been fully edited. Content may change prior to final publication. Citation information: DOI 10.1109/LWC.2021.3099867, IEEE Wireless Communications Letters

Dual-Polarized IRSs in Uplink MIMO-NOMA Networks: An Interference Mitigation Approach

Arthur S. de Sena, *Student Member*, *IEEE*, Pedro H. J. Nardelli, *Senior Member*, *IEEE*, Daniel B. da Costa, *Senior Member*, *IEEE*, Ugo S. Dias, *Senior Member*, *IEEE*, Petar Popovski, *Fellow*, *IEEE*, and Constantinos B. Papadias, *Fellow*, *IEEE*

***Abstract*—In this work, intelligent reflecting surfaces (IRSs) are optimized to manipulate signal polarization and improve the uplink performance of a dual-polarized multiple-input multiple-output (MIMO) non-orthogonal multiple access (NOMA) network. By multiplexing subsets of users in the polarization domain, we propose a strategy for reducing the interference load observed in the successive interference cancellation (SIC) process. To this end, dual-polarized IRSs are programmed to mitigate interference impinging at the base station (BS) in unsigned polarizations, in which the optimal set of reflecting coefficients are obtained via conditional gradient method. We also develop an adaptive power allocation strategy to guarantee rate fairness within each subset, in which the optimal power coefficients are obtained via a low-complexity alternate approach. Our results show that all users can reach high data rates with the proposed scheme, substantially outperforming conventional systems.**

***Index Terms*—IRS, multi-polarization, MIMO, NOMA.**

I. Introduction

Dual-polarized antenna arrays are effective for overcoming physical space limitations in multiple-input multiple-output (MIMO) systems [1]. By organizing dual-polarized antennas into co-located pairs, one can double the number of antennas in arrays with the same dimensions as those used in single-polarized schemes. Dual-polarized MIMO systems can also deliver improved user multiplexing and higher spectral efficiency than that achieved in single-polarized counterparts [2]. Power-domain non-orthogonal multiple access (NOMA) is another promising technique envisioned for enabling massive access in future wireless systems. In the uplink, through successive interference cancellation (SIC), NOMA enables the base station (BS) to decode the messages coming simultaneously from different users, thereby leading to latency and spectral improvements. NOMA and dual-polarized MIMO combined render even larger gains that substantially outperform conventional systems [3]. Nevertheless, dual-polarized MIMO-NOMA schemes also come with some impairments.

In the uplink SIC process, the symbols from users with strong channel gains are decoded first while treating the messages from the weak ones as interference. The drawback is that the rates of strong users are always capped due to interference from the weak ones. Besides limiting the sum-rate, this behavior leads to unbalanced individual rates, which is not suitable for applications where multiple devices require a uniform performance. One can alleviate this issue by balancing the users' rates through adaptive power allocation [4]. However, since these schemes usually lead to excessive penalties for some users, the sum-rate is also impacted. Therefore, new strategies for alleviating SIC interference are necessary.

Fortunately, a dual-polarized intelligent reflecting surface (IRS) has recently emerged as a disruptive technology for optimizing the propagation environment [5]. In this work, we exploit dual-polarized IRSs to propose a novel approach for reducing the interference levels of the SIC process in the uplink. Specifically, we consider a multi-group dual-polarized MIMO-NOMA network where users and the BS employ dual-polarized antennas. Users within each group are subdivided into two subsets, in which the messages coming from each subset are received by the BS using only one polarization (or vertical or horizontal). To enable this scheme, each group is assisted by one dual-polarized IRS that is optimized to mitigate interference impinging on unassigned polarizations. We transform the complicated formulated problem into least squares sub-problems with ℓ_∞ norm constraints, and we show that they can be optimally solved via the Conditional Gradient method, based on which an iterative algorithm is proposed. By relying on the concept of signal alignment, we design precoding and reception vectors to align the signals of users from each subset into a common interference subspace. Furthermore, we optimize the power allocation to balance the rates of users within each subset. Among other insightful remarks, our results show that all users can reach high data rates with the proposed scheme, substantially outperforming conventional systems.

Notation: Bold-faced lower-case letters denote vectors and upper-case denote matrices. The transpose and the Hermitian transpose of $\mathbf{A}$ are represented by $\mathbf{A}^T$ and $\mathbf{A}^H$, respectively. The symbol $\odot$ represents the Khatri-Rao product [6], $\mathbf{I}_M$ is the identity matrix of dimension $M \times M$, and $\mathbf{0}_{M,N}$ is the $M \times N$ matrix with all zero entries. The operator $\mathrm{vec}(\cdot)$ transforms a $M \times N$ matrix into a column vector of length MN, $\mathrm{vecd}(\cdot)$ converts the diagonal elements of an $M \times M$ square matrix into a column vector of length M, and $\mathrm{diag}(\cdot)$ transforms a vector of length M into an $M \times M$ diagonal matrix.

II. System Model

Consider that multiple users are communicating in uplink mode with a single BS in a MIMO-NOMA network. The BS and the users employ multiple antennas organized into co-located pairs, with each pair comprising antenna elements with orthogonal polarizations, i.e., vertical and horizontal

A. S. de Sena and P. H. J. Nardelli are with Lappeenranta–Lahti University of Technology, Finland, (email: arthur.sena@lut.fi, pedro.nardelli@lut.fi). D. B. da Costa is with the National Yunlin University of Science and Technology, Taiwan, and with the Federal University of Ceará, Brazil (email: danielbcosta@ieee.org). U. S. Dias is with the University of Brasília, Brazil (email: ugodias@ieee.org). P. Popovski is with Aalborg University, Denmark (email: petarp@es.aau.dk). C. B. Papadias is with the American College of Greece, Greece (email: cpapadias@acg.edu). This work is partly supported by the Academy of Finland n.319009, 321265, n.328869 and CHIST-ERA-17-BDSI-003/n.326270.

This article has been accepted for publication in a future issue of this journal, but has not been fully edited. Content may change prior to final publication. Citation information: DOI 10.1109/LWC.2021.3099867, IEEE Wireless Communications Letters

polarizations. The number of antenna pairs at the BS is denoted by $M/2$, and at the users by $N/2$, in which, due to the dual-polarized antenna structure, we assume that M and N are even and greater than 2. Moreover, the users are clustered into G groups with U users each. As mentioned, the performance of NOMA is limited by interference. To alleviate this major issue, we exploit the concepts of a dual-polarized IRS to propose a novel strategy. First, we assume that one IRS with L dual-polarized reflecting elements is installed between each group and the BS, i.e., there are G IRSs. Second, the BS subdivides each group into 2 subsets, in which vertically polarized antennas are assigned to receive the messages from the first subset, that contains U^v users, and horizontally polarized antennas are assigned to the second subset, that contains U^h users, such that $U^v + U^h = U$. Then, the IRSs are optimized to ensure that the signals coming from each subset impinge only at antennas corresponding to the assigned polarization. This scheme is illustrated in Fig. 1.

The phases and amplitude of reflection induced by the dual-polarized IRS for the gth group can be organized in the following block diagonal matrix [5]

$$\mathbf{\Theta}_g = \begin{bmatrix} \mathbf{\Phi}_g^{vv} & \mathbf{\Phi}_g^{hv} \\ \mathbf{\Phi}_g^{vh} & \mathbf{\Phi}_g^{hh} \end{bmatrix} \in \mathbb{C}^{2L \times 2L}, \tag{1}$$

where $\mathbf{\Phi}_g^{pq} = \mathrm{diag}\{[\alpha_{g,1}^{pq} e^{-j\phi_{g,1}^{pq}}, \cdots, \alpha_{g,L}^{pq} e^{-j\phi_{g,L}^{pq}}]\} \in \mathbb{C}^{L \times L}$, with $\phi_{g,l}^{pq}$ and $\alpha_{g,l}^{pq}$ representing, respectively, the phase and amplitude of reflection induced by the lth IRS element[1] from polarization p to polarization q, with $p, q \in \{v, h\}$ (v stands for vertical and h for horizontal). Given the matrix in (1), we can represent the full channel matrix obtained at the BS by

$$\mathbf{H}_{gu} = \begin{bmatrix} \mathbf{F}_g^{vv} & \mathbf{0}_{L,\frac{M}{2}} \\ \mathbf{0}_{L,\frac{M}{2}} & \mathbf{F}_g^{hh} \end{bmatrix}^H \begin{bmatrix} \mathbf{\Phi}_g^{vv} & \mathbf{\Phi}_g^{hv} \\ \mathbf{\Phi}_g^{vh} & \mathbf{\Phi}_g^{hh} \end{bmatrix} \begin{bmatrix} \mathbf{G}_{gu}^{vv} & \sqrt{\chi^{\text{U-IRS}}}\mathbf{G}_{gu}^{hv} \\ \sqrt{\chi^{\text{U-IRS}}}\mathbf{G}_{gu}^{vh} & \mathbf{G}_{gu}^{hh} \end{bmatrix} + \begin{bmatrix} \mathbf{D}_{gu}^{vv} & \sqrt{\chi^{\text{U-BS}}}\mathbf{D}_{gu}^{hv} \\ \sqrt{\chi^{\text{U-BS}}}\mathbf{D}_{gu}^{vh} & \mathbf{D}_{gu}^{hh} \end{bmatrix} \in \mathbb{C}^{M \times N}, \tag{2}$$

where $\mathbf{D}_{gu}^{pq} = \sqrt{\zeta_{gu}^{\text{U-BS}}}\tilde{\mathbf{D}}_{gu}^{pq} \in \mathbb{C}^{\frac{M}{2} \times \frac{N}{2}}$, $\mathbf{G}_{gu}^{pq} = \sqrt{\frac{\zeta_{gu}^{\text{U-IRS}}}{2}}\tilde{\mathbf{G}}_{gu}^{pq} \in \mathbb{C}^{L \times \frac{N}{2}}$, and $\mathbf{F}_g^{pq} = \sqrt{\zeta_{gu}^{\text{IRS-BS}}}\tilde{\mathbf{F}}_g^{pq} \in \mathbb{C}^{L \times \frac{M}{2}}$, with $\tilde{\mathbf{D}}_g^{pq}$, $\tilde{\mathbf{G}}_g^{pq}$ and $\tilde{\mathbf{F}}_g^{pq}$ modeling, respectively, the fast-fading channels between the uth user and the BS (link U-BS), the uth user and the gth IRS (link U-IRS), and the gth IRS and the BS (link IRS-BS), from the polarization p to the polarization q, in which the entries of $\tilde{\mathbf{D}}_g^{pq}$, $\tilde{\mathbf{G}}_g^{pq}$ and $\tilde{\mathbf{F}}_g^{pq}$ follow the complex Gaussian distribution with zero mean and unity variance. Moreover, $\zeta_{gu}^{\text{U-BS}}$, $\zeta_{gu}^{\text{U-IRS}}$, and $\zeta_{gu}^{\text{IRS-BS}}$ represent, respectively, the large-scale fading coefficients for the links U-BS, U-IRS, and IRS-BS, the normalization factor $\frac{1}{\sqrt{2}}$ ensures a passive beam splitting at the IRS, and $\chi^{\text{U-IRS}}$, and $\chi^{\text{U-BS}} \in [0, 1]$ denote the inverse of the cross-polar discrimination parameter (iXPD) that measures the power leakage between polarizations. Note that, for mathematical convenience, depolarization phenomena are not considered in the link IRS-BS. Further details for the channel modeling of dual-polarized IRSs can be found in [5].

Given the channel model in (2), the signal received at BS coming from all user groups can be expressed by

$$\mathbf{y} = \sum_{m=1}^{G} \sum_{n=1}^{U} \mathbf{H}_{mn}\mathbf{x}_{mn} + \mathbf{n} \in \mathbb{C}^M, \tag{3}$$

[1]Discrete reflection coefficients shall be considered in future works.

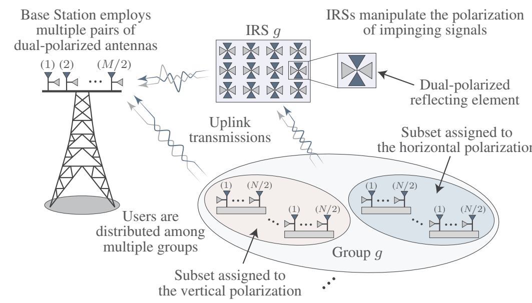

Fig. 1: System model. Each dual-polarized IRS mitigates polarization interference from one group of users.

where $\mathbf{x}_{mn} = \mathbf{p}_{mn}\sqrt{P\beta_{mn}}x_{mn} \in \mathbb{C}^N$, in which $\mathbf{p}_{mn}$ is a precoding vector to be explained later, P is the transmit power budget, $\beta_{mn} \in [0, 1]$ is the power allocation coefficient, x_{mn} represents the transmitted data symbol, and $\mathbf{n} = [(\mathbf{n}^v)^T, (\mathbf{n}^h)^T]^T \in \mathbb{C}^M$ is the noise vector observed at the BS, whose entries follow the complex Gaussian distribution with zero mean and variance σ_n.

III. IRS Optimization, Precoding, and Reception

A. IRS optimization

In this section, we focus on the optimization of the IRSs. Firstly, let us represent each subset by the index set $\mathcal{G}_g^p = \{1, 2, \cdots, U^p\}$, in which $p \in \{v, h\}$, and let:

$$\mathbf{G}_{gu}^v = \left[\mathbf{G}_{gu}^{vv} \; \sqrt{\chi^{\text{U-IRS}}}\mathbf{G}_{gu}^{hv}\right], \; \mathbf{G}_{gu}^h = \left[\sqrt{\chi^{\text{U-IRS}}}\mathbf{G}_{gu}^{vh} \; \mathbf{G}_{gu}^{hh}\right]$$
$$\mathbf{D}_{gu}^v = \left[\mathbf{D}_{gu}^{vv} \; \sqrt{\chi^{\text{U-IRS}}}\mathbf{D}_{gu}^{hv}\right], \; \mathbf{D}_{gu}^h = \left[\sqrt{\chi^{\text{U-IRS}}}\mathbf{D}_{gu}^{vh} \; \mathbf{D}_{gu}^{hh}\right].$$

Then, we can expand the signal model in (3) as follows

$$\mathbf{y} = \sum_{m=1}^{G}\left[\sum_{n=1}^{U}\left(\begin{bmatrix} (\mathbf{F}_m^{vv})^H \mathbf{\Phi}_m^{vv} \mathbf{G}_{mn}^v \\ (\mathbf{F}_m^{hh})^H \mathbf{\Phi}_m^{vh} \mathbf{G}_{mn}^v \end{bmatrix} + \begin{bmatrix} (\mathbf{F}_m^{vv})^H \mathbf{\Phi}_m^{hv} \mathbf{G}_{mn}^h \\ (\mathbf{F}_m^{hh})^H \mathbf{\Phi}_m^{hh} \mathbf{G}_{mn}^h \end{bmatrix}\right)\mathbf{x}_{mn} + \sum_{s \in \mathcal{G}_m^v} \begin{bmatrix} \mathbf{D}_{ms}^v \\ \mathbf{D}_{ms}^h \end{bmatrix} \mathbf{x}_{ms} + \sum_{t \in \mathcal{G}_m^h} \begin{bmatrix} \mathbf{D}_{mt}^v \\ \mathbf{D}_{mt}^h \end{bmatrix} \mathbf{x}_{mt}\right] + \mathbf{n}. \tag{4}$$

Following the proposed strategy, the messages transmitted from users in subset $\mathcal{G}_g^v$ should arrive at the BS only through the channels modeled by the upper blocks of the matrices in (4), while the messages from $\mathcal{G}_g^h$ should arrive only through the lower blocks, in both reflected, U-IRS-BS, and direct, U-BS, links. To this end, the IRS associated with the gth group must mitigate all transmissions from subset $\mathcal{G}_g^v$ that impinges the BS with horizontal polarization, and all transmissions from $\mathcal{G}_g^h$ that impinges the BS with vertical polarization.

Therefore, we can formulate the optimization problem as in (5), shown at the top of the next page. Due to the complicated matricial objective function, and the diagonal matrices constraint, solving problem (5) in its original form is challenging. Therefore, we recall the Khatri-Rao property $(\mathbf{C}^T \odot \mathbf{A})\mathrm{vecd}(\mathbf{B}) = \mathrm{vec}(\mathbf{ABC})$ [6] to transform (5) into a simpler equivalent problem. More specifically, we define:

$$\boldsymbol{\theta}_g^{pq} = \mathrm{vecd}(\mathbf{\Phi}_g^{pq}), \; \mathbf{z}_g^v = \sum_{t \in \mathcal{G}_g^h} \mathbf{D}_{gt}^v \mathbf{x}_{gt}, \; \mathbf{z}_g^h = \sum_{s \in \mathcal{G}_g^v} \mathbf{D}_{gs}^h \mathbf{x}_{gs},$$

$$\mathbf{W}_g^{vv} = \left[\sum_{n=1}^{U} \mathbf{G}_{gn}^v \mathbf{x}_{gn}\right]^T \odot (\mathbf{F}_g^{vv})^H, \; \tilde{\mathbf{W}}_g^{vv} = \left[\sum_{n=1}^{U} \mathbf{G}_{gn}^h \mathbf{x}_{gn}\right]^T \odot (\mathbf{F}_g^{vv})^H,$$

$$\mathbf{W}_g^{hh} = \left[\sum_{n=1}^{U} \mathbf{G}_{gn}^h \mathbf{x}_{gn}\right]^T \odot (\mathbf{F}_g^{hh})^H, \; \tilde{\mathbf{W}}_g^{hh} = \left[\sum_{n=1}^{U} \mathbf{G}_{gn}^v \mathbf{x}_{gn}\right]^T \odot (\mathbf{F}_g^{hh})^H.$$

This article has been accepted for publication in a future issue of this journal, but has not been fully edited. Content may change prior to final publication. Citation information: DOI 10.1109/LWC.2021.3099867, IEEE Wireless Communications Letters

$$\underset{\substack{\boldsymbol{\Phi}_g^{vv},\boldsymbol{\Phi}_g^{vh},\\ \boldsymbol{\Phi}_g^{hv},\boldsymbol{\Phi}_g^{hh}}}{\arg\min} \left\| \begin{bmatrix} (\mathbf{F}_g^{vv})^H \boldsymbol{\Phi}_g^{vv} \sum_{n=1}^{U} \mathbf{G}_{gn}^{v}\mathbf{x}_{gn} \\ (\mathbf{F}_g^{hh})^H \boldsymbol{\Phi}_g^{vh} \sum_{n=1}^{U} \mathbf{G}_{gn}^{v}\mathbf{x}_{gn} \end{bmatrix} + \begin{bmatrix} (\mathbf{F}_g^{vv})^H \boldsymbol{\Phi}_g^{hv} \sum_{n=1}^{U} \mathbf{G}_{gn}^{h}\mathbf{x}_{gn} \\ (\mathbf{F}_g^{hh})^H \boldsymbol{\Phi}_g^{hh} \sum_{n=1}^{U} \mathbf{G}_{gn}^{h}\mathbf{x}_{gn} \end{bmatrix} + \begin{bmatrix} \sum_{t\in\mathcal{G}_g^h} \mathbf{D}_{gt}^{v}\mathbf{x}_{gt} \\ \sum_{s\in\mathcal{G}_g^v} \mathbf{D}_{gs}^{h}\mathbf{x}_{gs} \end{bmatrix} \right\|^2 \tag{5a}$$

$$\text{s.t.} \ |\omega_{g,l}^{pq}|^2 \le 1, \ \ \forall l \in [1, L], \forall p, q \in \{v, h\}, \tag{5b}$$

$$\boldsymbol{\Phi}_g^{vv}, \boldsymbol{\Phi}_g^{vh}, \boldsymbol{\Phi}_g^{hv}, \boldsymbol{\Phi}_g^{hh} \ \text{diagonal.} \tag{5c}$$

Then, (5) is transformed into the following sub-problems

$$\underset{\boldsymbol{\theta}_g^{vv},\boldsymbol{\theta}_g^{hv}}{\arg\min} \left\| \begin{bmatrix} \mathbf{W}_g^{vv} & \tilde{\mathbf{W}}_g^{vv} \end{bmatrix} \begin{bmatrix} \boldsymbol{\theta}_g^{vv} \\ \boldsymbol{\theta}_g^{hv} \end{bmatrix} + \mathbf{z}_g^{v} \right\|^2 \tag{6a}$$

$$\text{s.t.} \ \left\| \begin{bmatrix} \boldsymbol{\theta}_g^{vv} \\ \boldsymbol{\theta}_g^{hv} \end{bmatrix} \right\|_\infty \le 1, \tag{6b}$$

$$\underset{\boldsymbol{\theta}_g^{vh},\boldsymbol{\theta}_g^{hh}}{\arg\min} \left\| \begin{bmatrix} \tilde{\mathbf{W}}_g^{hh} & \mathbf{W}_g^{hh} \end{bmatrix} \begin{bmatrix} \boldsymbol{\theta}_g^{vh} \\ \boldsymbol{\theta}_g^{hh} \end{bmatrix} + \mathbf{z}_g^{h} \right\|^2 \tag{7a}$$

$$\text{s.t.} \ \left\| \begin{bmatrix} \boldsymbol{\theta}_g^{vh} \\ \boldsymbol{\theta}_g^{hh} \end{bmatrix} \right\|_\infty \le 1. \tag{7b}$$

The objective functions of the problems above are of the form $f(\boldsymbol{\theta}) = \|\mathbf{W}\boldsymbol{\theta} + \mathbf{z}\|^2$, which has gradient $\nabla f(\boldsymbol{\theta}) = 2\mathbf{W}^H(\mathbf{W}\boldsymbol{\theta} + \mathbf{z})$, and Hessian given by $2\mathbf{W}^H\mathbf{W}$. Consequently, since the Hessian matrix of $f(\boldsymbol{\theta})$ is positive semidefinite, the functions in (6a) and (7a) are convex. Moreover, the ℓ_∞ norm constraints in (6b) and (7b) define convex compact subsets in the Hilbert space. As a result, problems (6) and (7) can be solved via the Conditional Gradient method [7], which is implemented in Algorithm 1. The algorithm converges to the optimal solutions at a rate of $\mathcal{O}(\frac{1}{k})$, with k representing its iterations. Furthermore, since the optimization happens over the ℓ_∞ space, each iteration has linear time complexity [8].

In this paper, the BS is responsible for executing Algorithm 1 and sending the optimized reflecting coefficients to the IRSs (e.g., through a backhaul link). To this end, we assume perfect knowledge of the global channel state information (CSI).

B. Precoding for intra-group channel alignment

We build $\mathbf{p}_{gu}$ to align the channels of users within each subset. Specifically, we design $\mathbf{p}_{gu}$ to align only the channels corresponding to the assigned polarization of the link U-BS. For notation simplicity, let $\tilde{\mathbf{D}}_{gu}^{v} = (\sqrt{\zeta_{gu}^{\text{U-BS}}})^{-1}\mathbf{D}_{gu}^{v}$ and $\tilde{\mathbf{D}}_{gu}^{h} = (\sqrt{\zeta_{gu}^{\text{U-BS}}})^{-1}\mathbf{D}_{gu}^{h}$ be the block matrices corresponding to the fast-fading arriving at the BS antennas with vertical and horizontal polarizations, respectively. Then, for users in subset $\mathcal{G}_g^p$, with $p \in \{v, h\}$, the following must be achieved

$$\tilde{\mathbf{D}}_{g1}^{p}\mathbf{p}_{g1} = \tilde{\mathbf{D}}_{g2}^{p}\mathbf{p}_{g2} = \cdots = \tilde{\mathbf{D}}_{gU^p}^{p}\mathbf{p}_{gU^p}. \tag{8}$$

This goal can be obtained by solving the following problem

$$\begin{bmatrix} \mathbf{I}_{\frac{M}{2}} & -\tilde{\mathbf{D}}_{g1}^{p} & \mathbf{0}_{\frac{M}{2},N} & \cdots & \mathbf{0}_{\frac{M}{2},N} \\ \mathbf{I}_{\frac{M}{2}} & \mathbf{0}_{\frac{M}{2},N} & -\tilde{\mathbf{D}}_{g2}^{p} & \cdots & \mathbf{0}_{\frac{M}{2},N} \\ \vdots & \vdots & \vdots & \ddots & \vdots \\ \mathbf{I}_{\frac{M}{2}} & \mathbf{0}_{\frac{M}{2},N} & \mathbf{0}_{\frac{M}{2},N} & \cdots & -\tilde{\mathbf{D}}_{gU^p}^{p} \end{bmatrix} \begin{bmatrix} \bar{\mathbf{d}}_g^p \\ \mathbf{p}_{g1} \\ \vdots \\ \mathbf{p}_{gU^p} \end{bmatrix} = \mathbf{0}_{\left(U^p \frac{M}{2}\right),1}, \tag{9}$$

where $\bar{\mathbf{d}}_g^p \in \mathbb{C}^{\frac{M}{2}}$ is the aligned channel vector obtained by the BS at polarization p from users in subset $\mathcal{G}_g^p$, i.e., $\bar{\mathbf{d}}_g^p = \tilde{\mathbf{D}}_{gu}^{p}\mathbf{p}_{gu}, \forall u \in \mathcal{G}_g^p$. Moreover, note that since the matrix in the leftmost side of (9) has dimension $\left(\frac{M}{2}U^p\right) \times \left(\frac{M}{2} + NU^p\right)$, the constraint $2NU^p > M\left(U^p - 1\right)$ must be obeyed.

C. Inter-group interference cancellation

Since the channels of users assigned to the same polarization have been aligned, now we can compute the reception vector intended to remove inter-group interference. The desired vector for the receive polarization $p \in \{v, h\}$ can be derived as

$$\mathbf{q}_g^p = \text{null}\left\{ \left[\bar{\mathbf{d}}_1^p, \cdots, \bar{\mathbf{d}}_{(g-1)}^p, \bar{\mathbf{d}}_{(g+1)}^p, \cdots, \bar{\mathbf{d}}_G^p\right]^H \right\} \in \mathbb{C}^{\frac{M}{2}}, \tag{10}$$

where, to ensure the existence of a nontrivial null space, $M > 2(G-1)$ must be satisfied.

D. Signal reception

After filtering the signals received in both polarizations through the vector in (10), all inter-group interference vanishes. Therefore, from (4), the superimposed symbol from the gth group detected by the BS can be written as

$$\hat{\mathbf{x}}_g = \begin{bmatrix} (\mathbf{q}_g^v)^H \bar{\mathbf{d}}_g^v \sum_{s\in\mathcal{G}_g^v} \sqrt{\zeta_{gs}^{\text{U-BS}} P \beta_{gs}} x_{gs} \\ (\mathbf{q}_g^h)^H \bar{\mathbf{d}}_g^h \sum_{t\in\mathcal{G}_g^h} \sqrt{\zeta_{gt}^{\text{U-BS}} P \beta_{gt}} x_{gt} \end{bmatrix} + \begin{bmatrix} I_g^v \\ I_g^h \end{bmatrix} + \begin{bmatrix} (\mathbf{q}_g^v)^H \mathbf{n}^v \\ (\mathbf{q}_g^h)^H \mathbf{n}^h \end{bmatrix} \in \mathbb{C}^2, \tag{11}$$

where I_g^p is the polarization interference left by the gth IRS, which is defined by

$$\begin{bmatrix} I_g^v \\ I_g^h \end{bmatrix} = \sum_{n=1}^{U} \begin{bmatrix} (\mathbf{q}_g^v)^H (\mathbf{F}_g^{vv})^H \boldsymbol{\Phi}_g^{vv} \mathbf{G}_{gn}^{v}\mathbf{x}_{gn} \\ (\mathbf{q}_g^h)^H (\mathbf{F}_g^{hh})^H \boldsymbol{\Phi}_g^{vh} \mathbf{G}_{gn}^{v}\mathbf{x}_{gn} \end{bmatrix} + \sum_{n=1}^{U} \begin{bmatrix} (\mathbf{q}_g^v)^H (\mathbf{F}_g^{vv})^H \boldsymbol{\Phi}_g^{hv} \mathbf{G}_{gn}^{h}\mathbf{x}_{gn} \\ (\mathbf{q}_g^h)^H (\mathbf{F}_g^{hh})^H \boldsymbol{\Phi}_g^{hh} \mathbf{G}_{gn}^{h}\mathbf{x}_{gn} \end{bmatrix} + \begin{bmatrix} (\mathbf{q}_g^v)^H \sum_{t\in\mathcal{G}_g^h} \mathbf{D}_{gt}^{v}\mathbf{x}_{gt} \\ (\mathbf{q}_g^h)^H \sum_{s\in\mathcal{G}_g^v} \mathbf{D}_{gs}^{h}\mathbf{x}_{gs} \end{bmatrix}. \tag{12}$$

As one can observe, after filtering the received signals through the detection vectors, the BS retrieves two super-

---

Algorithm 1: Algorithm for optimizing the dual polarized IRSs based on the Conditional Gradient method

Input: $K, \mathbf{z}_g^v, \mathbf{z}_g^h, [\mathbf{W}_g^{vv}\ \tilde{\mathbf{W}}_g^{vv}], [\tilde{\mathbf{W}}_g^{hh}\ \mathbf{W}_g^{hh}]$.
Output: $\boldsymbol{\Phi}_g^{vv}, \boldsymbol{\Phi}_g^{hv}, \boldsymbol{\Phi}_g^{vh}, \boldsymbol{\Phi}_g^{hh}$.

Initialize $c = 1, \boldsymbol{\theta}_g^{(1)} = \mathbf{0}_{2L,1}, \tilde{\boldsymbol{\theta}}_g^{(1)} = \mathbf{0}_{2L,1}$;
for $k = 1$ *to* $K - 1$ **do**
  Compute the gradients of (6a) and (7a):
  $\nabla f(\boldsymbol{\theta}_g^{(k)}) = 2[\mathbf{W}_g^{vv}\ \tilde{\mathbf{W}}_g^{vv}]^H([\mathbf{W}_g^{vv}\ \tilde{\mathbf{W}}_g^{vv}]\boldsymbol{\theta}_g^{(k)} + \mathbf{z}_g^v)$,
  $\nabla f(\tilde{\boldsymbol{\theta}}_g^{(k)}) = 2[\tilde{\mathbf{W}}_g^{hh}\ \mathbf{W}_g^{hh}]^H([\tilde{\mathbf{W}}_g^{hh}\ \mathbf{W}_g^{hh}]\tilde{\boldsymbol{\theta}}_g^{(k)} + \mathbf{z}_g^h)$;
  Construct the direction-finding vectors $\mathbf{s}^{(k)}$ and $\tilde{\mathbf{s}}^{(k)}$ by computing: $[\mathbf{s}^{(k)}]_i = -c \cdot \nabla f(\boldsymbol{\theta}_g^{(k)})$, and $[\tilde{\mathbf{s}}^{(k)}]_i = -c \cdot \nabla f(\tilde{\boldsymbol{\theta}}_g^{(k)})$;
  Compute the step size: $\nu^{(k)} = \frac{2}{2+k}$;
  Update the vectors of reflecting coefficients:
  $\boldsymbol{\theta}_g^{(k+1)} = (1 - \nu^{(k)})\boldsymbol{\theta}_g^{(k)} + \nu^{(k)}\mathbf{s}^{(k)}$,
  $\tilde{\boldsymbol{\theta}}_g^{(k+1)} = (1 - \nu^{(k)})\tilde{\boldsymbol{\theta}}_g^{(k)} + \nu^{(k)}\tilde{\mathbf{s}}^{(k)}$;
end
Obtain the final set of coefficients:
$\boldsymbol{\Phi}_g^{vv} = \text{diag}\left(\left[\boldsymbol{\theta}_g^{(K)}\right]_{1:L}\right)$, $\boldsymbol{\Phi}_g^{vh} = \text{diag}\left(\left[\tilde{\boldsymbol{\theta}}_g^{(K)}\right]_{1:L}\right)$,
$\boldsymbol{\Phi}_g^{hv} = \text{diag}\left(\left[\boldsymbol{\theta}_g^{(K)}\right]_{(L+1):2L}\right)$, $\boldsymbol{\Phi}_g^{hh} = \text{diag}\left(\left[\tilde{\boldsymbol{\theta}}_g^{(K)}\right]_{(L+1):2L}\right)$.

This article has been accepted for publication in a future issue of this journal, but has not been fully edited. Content may change prior to final publication. Citation information: DOI 10.1109/LWC.2021.3099867, IEEE Wireless Communications Letters

imposed symbols, i.e., one symbol from each polarization. Observe that, if the IRSs completely eliminate the signals in unassigned polarizations, the interference term in (12) will vanish. Next, the BS employs SIC to recover the messages of users assigned to their corresponding polarization.

IV. SINR Analysis

Since both inter-group and inter-subset interference have been addressed, now the BS can securely apply SIC to each polarization separately. For this, the BS first sorts users from each subset in a descending order based on their large scale fading coefficient observed in the link U-BS, such that $\zeta_{g1}^{\text{U-BS}} > \zeta_{g2}^{\text{U-BS}} > \cdots > \zeta_{gU^p}^{\text{U-BS}}$. Then, the SIC decoding process is carried out following this order, i.e., the symbol from the uth user received in polarization p is decoded by treating the messages from the $U^p - u$ weaker users as interference. More specifically, the recovered symbol that was transmitted from the uth user in subset $\mathcal{G}_g^p$, can be written as

$$\hat{x}_{gu}^p = \underbrace{(\mathbf{q}_g^p)^H \bar{\mathbf{d}}_g^p \sqrt{\zeta_{gu}^{\text{U-BS}} P \beta_{gu}} x_{gu}}_{\text{Desired symbol}} + \underbrace{(\mathbf{q}_g^p)^H \bar{\mathbf{d}}_g^p \sum_{n=u+1}^{U^p} \sqrt{\zeta_{gn}^{\text{U-BS}} P \beta_{gn}} x_{gn}}_{\text{Interference from weaker users}} + \underbrace{I_g^p}_{\text{Polarization interference}} + \underbrace{(\mathbf{q}_g^p)^H \mathbf{n}^p}_{\text{Noise}}. \quad (13)$$

By knowing that $|(\mathbf{q}_g^p)^H \mathbf{n}^p|^2 = (\mathbf{q}_g^p)^H \mathbf{n}^p (\mathbf{n}^p)^H \mathbf{q}_g^p = \sigma_n^2$, and defining $\rho = \frac{P}{\sigma_n^2}$, the SINR for the uth in $\mathcal{G}_g^p$ is given by

$$\gamma_{gu}^p = \frac{|(\mathbf{q}_g^p)^H \bar{\mathbf{d}}_g^p|^2 \zeta_{gu}^{\text{U-BS}} \beta_{gu}}{|(\mathbf{q}_g^p)^H \bar{\mathbf{d}}_g^p|^2 \sum_{n=u+1}^{U^p} \zeta_{gn}^{\text{U-BS}} \beta_{gn} + |I_g^p|^2/P + 1/\rho}. \quad (14)$$

V. Power Allocation for Rate Fairness

In this section, we develop an adaptive power allocation policy for balancing the data rates of users within each subset. Our aim is to show that the proposed dual-polarized IRS-MIMO-NOMA scheme can achieve a high throughput even when fair power allocation is employed.

Since in practical systems only small groups of users are served with NOMA, we assume that each subset is formed by only two users, i.e., there is a total of 4 users per group. Moreover, we consider that the polarization interference term in (13) is negligible so that $I_g^p \approx 0$. As a result, the data rate observed when decoding the symbol of the first user from the gth subset assigned to polarization p can be written as

$$R_{g1}^p = \log_2 \left(1 + \frac{|(\mathbf{q}_g^p)^H \bar{\mathbf{d}}_g^p|^2 \zeta_{g1}^{\text{U-BS}} \rho \beta_{g1}}{|(\mathbf{q}_g^p)^H \bar{\mathbf{d}}_g^p|^2 \zeta_{g2}^{\text{U-BS}} \rho \beta_{g2} + 1} \right), \quad (15)$$

and for the second user as

$$R_{g2}^p = \log_2 \left(1 + |(\mathbf{q}_g^p)^H \bar{\mathbf{d}}_g^p|^2 \zeta_{g2}^{\text{U-BS}} \rho \beta_{g2} \right). \quad (16)$$

Then, our goal can be accomplished by solving the following optimization problem:

$$\begin{aligned} &\arg\max_{\beta_{g1}, \beta_{g2}} \quad R_{g1}^p && (17a)\\ &\text{s.t.} \quad R_{g2}^p \geq R_{g1}^p, && (17b)\\ &\quad 0 \leq \beta_{g1} \leq 1, && (17c)\\ &\quad 0 \leq \beta_{g2} \leq 1, && (17d) \end{aligned}$$

where the objective function in (17a) aims at the maximization of the rate of the strong user, while the constraint (17b) ensures that the rate of the weak user does not drop below that achieved for the strong one, i.e., it guarantees fairness. Moreover, constraints (17c) and (17d) define the feasible set for the power allocation coefficients β_{g1} and β_{g2}.

Since the objective function in (17a) is an increasing function of β_{g1}, if we consider a fixed β_{g2}, (17) will be maximized when β_{g1} reaches the maximum value in the feasible set. Also, since $\log_2(\cdot)$ is a monotonic increasing function of its argument, the constraint (17b) can be equivalently represented by $|(\mathbf{q}_g^p)^H \bar{\mathbf{d}}_g^p|^2 \zeta_{g2}^{\text{U-BS}} \rho \beta_{g2} \geq \frac{|(\mathbf{q}_g^p)^H \bar{\mathbf{d}}_g^p|^2 \zeta_{g1}^{\text{U-BS}} \rho \beta_{g1}}{|(\mathbf{q}_g^p)^H \bar{\mathbf{d}}_g^p|^2 \zeta_{g2}^{\text{U-BS}} \rho \beta_{g2} + 1}$. With these observations, first, we consider β_{g1} to be a constant and optimize (17) in terms of only β_{g2}. More specifically, after simplifying (17b), we can write

$$\begin{aligned} &\arg\max_{\beta_{g2}} \quad \log_2 \left(1 + \frac{|(\mathbf{q}_g^p)^H \bar{\mathbf{d}}_g^p|^2 \zeta_{g1}^{\text{U-BS}} \rho \beta_{g1}}{|(\mathbf{q}_g^p)^H \bar{\mathbf{d}}_g^p|^2 \zeta_{g2}^{\text{U-BS}} \rho \beta_{g2} + 1} \right) && (18a)\\ &\text{s.t.} \left(|(\mathbf{q}_g^p)^H \bar{\mathbf{d}}_g^p|^2 \zeta_{g2}^{\text{U-BS}} \rho \right)^2 \beta_{g2}^2 + \left(|(\mathbf{q}_g^p)^H \bar{\mathbf{d}}_g^p|^2 \zeta_{g2}^{\text{U-BS}} \rho \right) \beta_{g2} \\ &\quad - \left(|(\mathbf{q}_g^p)^H \bar{\mathbf{d}}_g^p|^2 \zeta_{g1}^{\text{U-BS}} \rho \right) \beta_{g1} \geq 0, && (18b)\\ &\quad 0 \leq \beta_{g2} \leq 1. && (18c) \end{aligned}$$

One can verify that the second derivative of the objective function in (18a) is positive $\forall \beta_{g2} > 0$, which means convexity. Moreover, (18a) is a decreasing function of β_{g2}, which tells us that, if the constraint (18b) is relaxed, the global maximum within the feasible set is reached when $\beta_{g2} \to 0$. Also, note that (18b) is a concave upward quadratic function that increases with β_{g2}. Therefore, the solution for (18) can be obtained by computing the minimum possible value for β_{g2}, which clearly can be accomplished through the roots of (18b). However, for computing the desired roots, we need first to determine the value of β_{g1} in a way that β_{g2} can satisfy (18c). By noticing that (18b) is a decreasing function of β_{g1}, we optimize both coefficients with a simple alternate approach: first, aiming the maximization of R_{g1}^p, we initialize β_{g1} with 1. Then, we calculate the positive root of (18b) as in (19), shown at the top of the next page, and test if $\Delta_{g2} \leq 1$. If this is satisfied, then $\beta_{g2}^* = \Delta_{g2}$, and $\beta_{g1}^* = 1$. Otherwise, $\beta_{g2}^* = 1$, and β_{g1}^* is computed with (19) by setting $\Delta_{g2} = 1$.

VI. Simulation Results and Discussions

In this section, we evaluate the performance of the proposed IRS-MIMO-NOMA system. The conventional single-polarized MIMO-NOMA and MIMO with time division multiple access (TDMA) are used as baseline schemes. We consider a scenario with $G = 2$ groups of $U = 4$ users, in which, in both dual-polarized and single-polarized systems, the BS and the users employ $M = N = 4$ antennas. Given that the signal alignment approach from Section III successfully eliminates all inter-group interference, without loss of generality, we focus on the first group, and we assume that users 1, 2, 3, and 4 are located, respectively, at $d_1 = 20$ m, $d_2 = 40$ m, $d_3 = 80$ m, and $d_4 = 120$ m from the BS. Users 1 and 2 are assigned to the vertical polarization, and users 3 and 4 to the horizontal polarization. For simplicity, we assume that the distances between the users and the connected IRS are the same as that from the users to the BS. On the other hand, the distance between the IRS and the BS, denoted by $\bar{d}$, varies throughout the simulation

$$\Delta_{g2} = \left(-|(\mathbf{q}_g^p)^H \bar{\mathbf{d}}_g^p|^2 \zeta_{g2}^{\text{U-BS}} \rho + \sqrt{\left(|(\mathbf{q}_g^p)^H \bar{\mathbf{d}}_g^p|^2 \zeta_{g2}^{\text{U-BS}} \rho\right)^2 + 4 \left(|(\mathbf{q}_g^p)^H \bar{\mathbf{d}}_g^p|^2 \zeta_{g2}^{\text{U-BS}} \rho\right)^2 |(\mathbf{q}_g^p)^H \bar{\mathbf{d}}_g^p|^2 \zeta_{g1}^{\text{U-BS}} \rho \beta_{g1}} \right) \left(2 \left(|(\mathbf{q}_g^p)^H \bar{\mathbf{d}}_g^p|^2 \zeta_{g2}^{\text{U-BS}} \rho\right)^2 \right)^{-1}. \quad (19)$$

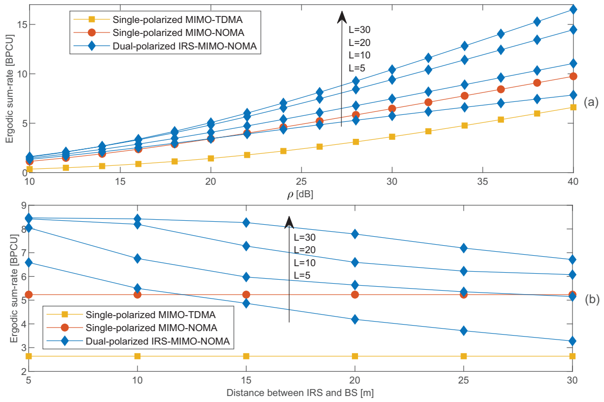

Fig. 2: Ergodic sum-rates with fixed power allocation when the IRS is located at $\bar{d} = 15$ m from the BS (a), and when ρ is fixed to 26 dB (b).

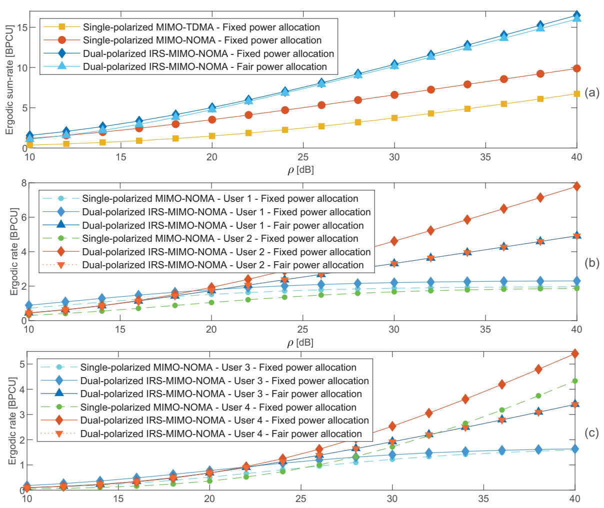

Fig. 3: Ergodic sum-rates (a) and rates (b)-(c) with fixed and fair power allocation for $L = 30$ and $\bar{d} = 10$ m.

examples. As a result, the large scale fading coefficients for the links U-BS and U-IRS are obtained by $\zeta_u^{\text{U-BS}} = \zeta_u^{\text{U-IRS}} = \delta d_u^{-\eta}$, and for the link IRS-BS by $\zeta_u^{\text{IRS-BS}} = \bar{d}^{-\eta}$, where δ is a gain set to 30 dB, and η is the path-loss exponent set to 2. Moreover, we set $\chi^{\text{U-BS}} = \chi^{\text{U-IRS}} = 0.5$, $P = 1$, and, in results with fixed power allocation, we assume that all users transmit using their total power, i.e., $\beta_1 = \beta_2 = \beta_3 = \beta_4 = 1$.

Fig. 2(a) compares the ergodic sum-rates of conventional MIMO-NOMA and MIMO-TDMA systems with those obtained with the dual-polarized IRS-MIMO-NOMA scheme for different numbers of reflecting elements when the IRS is deployed at 15 m from the BS. We can see that impressive gains can be achieved over the baseline schemes when the IRS becomes large enough. Fig. 2(b) shows the impact of the distance between the IRS and the BS on the system sum-rate for $\rho = 26$ dB. As can be noticed, the sum-rate of the IRS-MIMO-NOMA system decreases with the increase of the distance. Such behavior is explained by the fact that the IRS's ability to cancel polarization interference worsens when the distance increases. Despite that, for $L = 20$ and $L = 30$, the proposed scheme is able to outperform the conventional systems even when $\bar{d} = 30$ m.

Fig. 3(a) shows how the fair power allocation policy performs in terms of sum-rate. As one can see, because the fair policy decreases the data rates of some users to improve the rates of others, the fair IRS-MIMO-NOMA scheme experiences a sum-rate slightly inferior to the achieved with the fixed policy. Nevertheless, the fair scheme can still outperform all the baseline systems. For instance, the proposed scheme under fair power allocation surpasses 16 bits per channel use (BPCU) when $\rho = 40$ dB, which is more than 6 BPCU higher than that achieved by the single-polarized MIMO-NOMA, and incredibly 9 BPCU above that of MIMO-TDMA. Finally, Figs. 3(b) and 3(c) reveal the behavior of the rates observed for each user with fixed and fair power allocation. One can see that, in the IRS-MIMO-NOMA scheme, the rates of all users are improved, remarkably outperforming the conventional systems. The main reason for these improvements is that SIC is employed in each subset separately, which leads users to experience less interference in the decoding process. We can also verify that fair power allocation is highly beneficial to strong users. For instance, when $\rho = 40$ dB, while the rate of user 3 is limited to 1.63 BPCU in the IRS-MIMO-NOMA scheme with fixed policy, with fair power allocation, the same user can improve its rate to 3.39 BPCU.

VII. Conclusions

We have presented in this paper a novel approach for mitigating interference in the uplink of IRS-assisted dual-polarized MIMO-NOMA networks. The IRSs were optimized to mitigate interference impinging on unsigned polarizations at the BS, in which an iterative algorithm for computing the optimal set of reflecting coefficients was proposed. Furthermore, we exploited the concept of signal alignment to efficiently eliminate inter-group interference and developed an effective optimal power allocation to improve fairness in the network. Numerical results were presented to demonstrate the performance superiority of the proposed scheme.

References

[1] H. Asplund, *et al.*, *Advanced antenna systems for 5G network deployments*. Academic Press, 2020.
[2] J. Park and B. Clerckx, “Multi-user linear precoding for multi-polarized massive MIMO system under imperfect CSIT,” *IEEE Trans. Wireless Commun.*, vol. 14, no. 05, May 2015.
[3] A. S. de Sena, D. B. da Costa, Z. Ding, and P. H. J. Nardelli, “Massive MIMO-NOMA networks with multi-polarized antennas,” *IEEE Trans. Wireless Commun.*, vol. 18, no. 12, pp. 5630–5642, Dec. 2019.
[4] A. S. de Sena, F. R. M. Lima, D. B. da Costa, Z. Ding, P. H. J. Nardelli, U. S. Dias, and C. B. Papadias, “Massive MIMO-NOMA networks with imperfect SIC: Design and fairness enhancement,” *IEEE Trans. Wireless Commun.*, vol. 19, no. 9, pp. 6100–6115, Jun. 2020.
[5] A. S. de Sena, P. H. J. Nardelli, D. B. da Costa, F. R. M. Lima, L. Yang, P. Popovski, Z. Ding, and C. B. Papadias, “IRS-assisted massive MIMO-NOMA networks: Exploiting wave polarization,” *IEEE Trans. Wireless Commun.*, pp. 1–1, 2021.
[6] J. Brewer, “Kronecker products and matrix calculus in system theory,” *IEEE Trans. Circuits Syst.*, vol. 25, no. 9, pp. 772–781, 1978.
[7] D. Liu, K. Sun, Z. Wang, R. Liu, and Z. J. Zha, “Frank-Wolfe network: An interpretable deep structure for non-sparse coding,” *IEEE Trans. Circuits Syst. Video Technol.*, vol. 30, no. 9, pp. 3068–3080, 2020.
[8] M. Jaggi, “Revisiting Frank-Wolfe: Projection-free sparse convex optimization,” in *Proc. Int. Conf. Mach. Learn.*, vol. 28, 2013, pp. 427–435.